Fate of the Amino Acid in Glucose−Glycine Melanoidins Investigated by Solid-State Nuclear Magnetic Resonance (NMR)

Xiaowen Fang and Klaus Schmidt-Rohr*

Department of Chemistry, Iowa State University, Ames, Iowa 50011

The fate of the amino acid in the model Maillard reaction between glucose and glycine in a 1:1 molar ratio has been investigated by applying advanced ^{13}C and ^{15}N solid-state nuclear magnetic resonance (NMR) techniques to ^{13}C- and ^{15}N-labeled melanoidins formed in dry and solution reactions. Quantitative ^{13}C NMR shows that ~23% of carbon is from glycine; the ~2% loss compared to the 25% glycine C in the reactants is due to the COO moiety being liberated as CO_2 (Strecker degradation). ^{13}C J-modulation experiments on melanoidins made from doubly ^{13}C-labeled glycine show that the C−C backbone bond of about two-thirds of the incorporated amino acid stays intact, and about half of all glycine is incorporated as N−CH_2−COO without fragmentation. Degradation processes without CO_2 loss affect about one-eighth of glycine in dry reaction and about one-fourth in solution. These results indicate that Strecker degradation affects about one-fourth (dry reaction) to one-third (in solution) of all glycine but is not the main pathway of glycine incorporation. Spectra of Strecker degradation products show that C2 of glycine reacts to form N−CH_3, C−CH_n−C, or aromatic units, but not pyrazines or pyridines. The gycine-C1 carbon incorporated into the melanoidins remains ≥90% part of COO moieties; ~5% of amides have also been detected. The C2−N bond stays intact for ~70% of the incorporated glycine. The ^{15}N spectra show many peaks, over a 200 ppm range, documenting a multitude of different chemical environments of nitrogen, but no enamines or imines. The majority (>78%) of nitrogen, in particular most pyrrolic N, is not protonated. Because N−H predominates in amino acids and proteins, nonprotonated nitrogen may be a characteristic marker of Maillard reaction products.

KEYWORDS: Maillard reaction; Strecker degradation; melanoidin; solid-state NMR

INTRODUCTION

The Maillard reaction of reducing sugars with amine compounds (e.g., amino acids) is a classical nonenzymatic browning reaction (*1−5*) that is of significant interest in various fields (*2,6*). In food science, it is ubiquitous, with the formation of caramel candy from sugar and milk protein and the baking of cookies from sugar and egg protein as particularly pertinent examples. In medicine, it has been considered in diabetes and aging-related diseases (*6−8*). In environmental science, the Maillard reaction is commonly invoked to account for abiotic chemical transformations of organic matter (*9−13*).

Despite their common occurrence, the structure of most of the end products of the Maillard reaction, in particular the high molecular weight or insoluble melanoidins that account for most of the mass, has remained contentious (*4, 10, 11, 14−18*). Structural studies of melanoidins based on thermal degradation (*18−20*) indicate the presence of heterocycles, but do not provide absolute quantification of the components, and the results depend significantly on the degradation conditions (*19, 20*). Other studies are mainly based on elemental analysis of melanoidins, (*17, 21*),

which does not reveal connectivities between atoms. The most comprehensive structural information has come from ^{13}C and ^{15}N NMR investigations (*10, 11, 15, 16, 22*), which have provided an overall impression of the composition. Nevertheless, some peak assignments, for example, of the dominant peak in the ^{15}N spectrum (*10, 16*), have remained contentious, smaller bands have not been assigned at all, and quantification was rarely attempted. In addition, the simple NMR method used (cross-polarization) did not provide quantitative spectra, connectivities between atoms were not probed, and the spectra did not reveal to what extent and how the "backbone", that is, N−C1−C2, of the amino acid is incorporated into the melanoidins. Also as a result of limited structural knowledge, few clear molecular characteristics to distinguish Maillard reaction products from other types of natural organic matter have been identified.

In this paper, we apply advanced solid-state NMR to melanoidins made from glucose and isotopically labeled glycine in 1:1 molar ratio according to the standard procedures of the European COST Action 919 for the solvent-free reaction between glycine and glucose (*5, 19, 20, 23*). In particular, we follow the chemical fate of the amino acid, which is relatively simple compared with the transformations of the sugar. The most frequently discussed reaction of the amino acid in the Maillard

*Corresponding author [e-mail srohr@iastate.edu; telephone (515) 294-6105; fax (515) 294-0105].

reaction is Strecker degradation, by which the amino acid is broken up into CO_2, which is released from the material, an aldehyde, and ammonia, which may be liberated or reintegrated with sugar carbons to form a variety structures. The reported extent to which glycine atoms are incorporated into melanoidins via Strecker degradation has varied widely, between 0 and 65% (*21, 24*), probably depending on the reaction conditions. We quantify to what extent Strecker degradation and other types of fragmentation occur in Maillard reactions under dry heating and in solution. Furthermore, we characterize the degradation products, showing that enamines, imines, and pyrazines are not significant components of our melanoidins, whereas regular amines, which have not been recorded significantly in degradation studies (*19, 20*), are detected prominently in NMR. Modern multinuclear and multidimensional NMR of suitably [13]C- or ^{15}N-labeled compounds can elucidate the type, amount, and connectivity of carbons and nitrogens introduced into the melanoidin from a specific site in a reactant. Quantitative ^{13}C NMR and a technique for selecting isolated ^{13}C spins in a melanoidin produced from doubly ^{13}C-labeled glycine enable us to assess the occurrence of fragmentation at the C−C bond of glycine, whereas fragmentation at the C−N bond and the structure of degradation products is probed by various [15]N−[13]C experiments. To quantify NH_n versus nonprotonated tertiary N_t, we have performed both [15]N- and ^{13}C-detected [15]N{[1]H} dipolar dephasing experiments.

The experiments provide a comprehensive picture of the fate of glycine carbons and nitrogen in the Maillard reaction in both dry and solution conditions and demonstrate the level of quantitative detail that can be reached by modern NMR. Furthermore, our results indicate that nonprotonated N is a potential characteristic marker of melanoidins that distinguishes them from other common N-containing molecules such as proteins, amino acids, and amino sugars.

EXPERIMENTAL PROCEDURES

Materials. D-Glucose, anhydrous 99+%, and glycine, 98%, were purchased from Acros Organics. D-Glucose (U-[13]C_6, 99%, CLM-1396-1) and four labeled glycines (1-^{13}C, 99%, CLM-422-1; 2-^{13}C, 99%, CLM-136-1; 1,2-[13]C_2, CLM-1017; and ^{15}N, 98%, NLM-202-1) were obtained from CIL Inc. Glycine-2-[13]C−[15]N (99 atom % [13]C, 98+ atom % [15]N) was obtained from Isotec. If not otherwise mentioned, the following chemicals were of ACS grade and were purchased from Fisher Scientific: $NaH_2PO_4 \cdot H_2O$, $Na_2HPO_4 \cdot 7H_2O$, Na_2CO_3. The dialysis tubing from Fisherbrand was made of regenerated cellulose with a nominal MWCO of 6000−8000, with volume/length = 5.10 mL/cm. Filter papers were 41 ashless from Whatman. Water was E-pure water (Barnstead).

Synthesis of Melanoidin: Dry Reaction. Following European COST Action 919 (*23*) and refs *5*, *19*, and *20*, an equimolar mixture of glucose and glycine (5.6 mmol each) was dissolved in 15 mL of E-pure water in a scintillation vial and was freeze-dried for 1 day using a lyophilizer (Labconco Freezon 4.5). The dried sample in the scintillation vial was heated in a closed preheated oven (VMR Scientific Products, model 1430) at 125 °C for 2 h. After 2 h of heating, the color of the sample turned to dark brown and its volume increased. When cooled to room temperature in a desiccator, the sample was dissolved into 100 mL of E-pure water, with magnetic stirring for 1 h to dissolve as much sample as possible. Then the solution was filtered twice through filter paper, and the filtrate was collected and transferred into 30 cm long dialysis tubing. The tubing was submerged in 2 L of E-pure water at 4 °C. Every 12 h, the water surrounding the dialysis tubing was replaced with fresh water (2000 mL) for four times total. After 48 h of dialysis, the solution in the tubing was collected and freeze-dried. This soluble high molecular weight (HMW) fraction was analyzed here, following ref *19* for comparison with the corresponding fraction in the solution reaction. It accounts for ∼7% of reactant mass. The insoluble fraction, which is the main product (∼50% yield), shows ^{13}C and ^{15}N NMR spectra similar to those of the HMW fraction studied here.

Synthesis of Melanoidin: Solution Reaction. Following refs *25* and *11*, a 500 mL flask containing 100 mL of solution of D-glucose and glycine (0.056 M each) dissolved in a pH 8 buffer solution was sealed and heated in a preheated oven at 100 °C for 1 week. After the first 48 h, the color of the solution turned brown and the pH dropped to ∼5. $Na_2HPO_4 \cdot 7H_2O$ was added to adjust the pH back to 8.5 at room temperature. Another 5 days of reaction caused the pH of the solution to drop to < 6. The remaining steps (filtering, dialysis, and freeze-drying) were the same as for the dry-reaction products. The yield for the HMW fraction was ∼20%; no insoluble fraction was obtained under these reaction conditions.

NMR Parameters. Solid-state magic-angle spinning (MAS) NMR experiments were performed at room temperature using a Bruker DSX 400 spectrometer at 400 MHz for ^{1}H, 100 MHz for ^{13}C, and 40 MHz for ^{15}N, using a Bruker 4 mm triple-resonance MAS probe head. ZrO_2 rotors (4 mm diameter) were used with a 5 mm long glass insert at the bottom to constrain the sample to within the radio frequency coil. [13]C and ^{1}H chemical shifts were referenced to TMS, using the COO^- resonance of α-glycine at 176.49 ppm as a secondary reference for ^{13}C, and the NIST hydroxyapatite proton peak at 0.18 ppm as a secondary reference for [1]H. The ^{15}N chemical shifts were referenced to liquid ammonia by setting the *N*-acetylvaline peak to 122 ppm. The 90° pulse length was 4 μs for both ^{13}C and [1]H. Two-pulse phase modulation (TPPM) decoupling on the ^{1}H channel was applied during ^{13}C or ^{15}N signal detection.

CP/TOSS NMR. For routine analysis of unlabeled and labeled samples, [1]H−[13]C cross-polarization (CP) combined with four-pulse total suppression of spinning sidebands (TOSS) (*26*) spectra were acquired at 6.5 kHz MAS. The CP contact time was 1 ms, and the recycle delay was 3 s.

High-Speed Quantitative ^{13}C DP/Echo/MAS NMR. To quantify the percentages of glycine-C1 and -C2 in the melanoidins, quantitative ^{13}C direct polarization (DP)/MAS NMR spectra were acquired for the samples produced from singly or doubly glycine-^{13}C labeling reactants at 14 kHz MAS. A Hahn echo requiring two rotation periods was used before detection to avoid baseline distortions. To avoid T_2 relaxation and line broadening of CH_2 signals, sufficiently strong ($\gamma B_1/2\pi > 70$ kHz) TPPM decoupling (*27*) was found to be necessary. The recycle delays were estimated by measuring $CP/T_1/TOSS$ spectra with two or three different T_1 filter times. The T_1 filter time that reduced all carbon signals to < ∼5% of the full intensity was chosen as the recycle delay of the quantitative DP/echo/MAS experiment, which ensures that all carbons are fully relaxed. More details are given in ref *28*.

Two-Dimensional Separation of Undistorted Chemical Shift Anisotropy Powder Patterns (SUPER). The two-dimensional SUPER NMR method was applied to the glycine-[13]C1 labeled melanoidins to elucidate the chemical structure of the COO groups. The ^{13}C chemical shift anisotropy powder pattern of COOC is different from that of COOH or COO^- because of their different electronic environments. By the 2D SUPER technique, the powder pattern can be measured for each isotropic chemical shift. During each t_1 rotation period, two 720° pulses (consisting of four 180° pulses) on the ^{13}C channel were applied symmetrically to recouple the chemical shift anisotropy. More details regarding the principle of SUPER pulse sequence and the powder patterns of different carbon functional groups can be found in ref *29*. A cross-polarization time of 1 ms was used, at a spinning frequency of 5 kHz. The increment of the evolution time t_1 was one rotation period (e.g., $t_r = 200\,\mu$s at 5 kHz MAS).

CH_2 Spectral Editing. Spectral editing of CH_2 signals was achieved by selection of the three-spin coherence of CH_2 groups, using a [13]C 90° pulse and [1]H 0°/180° pulses applied after $t_r/4$ with MREV-8 decoupling. (*30*) The MAS frequency was 5.787 kHz.

J_{CC}-Dephasing: Isolated ^{13}C versus [13]C−[13]C Spin-Pairs. After the Maillard reaction, the chemical bond connectivity of C1−C2 of glycine was determined using J_{CC}-modulation solid echo pulse sequence (see Figure S1 of the Supporting Information). In this pulse sequence, after 90° pulse excitation (or cross-polarization) of ^{13}C, heteronuclear TPPM decoupling is turned on. On the ^{13}C channel, two back-to-back 45° pulses divide a total period of ∼10 ms (= 68 t_r at a MAS frequency of 7 kHz) into two parts before detection(*31*). Two 180° pulses were placed in the middle of each part to refocus isotropic chemical shift evolution. When the two 45° pulses are of the same phase, a solid echo is generated to refocus the evolution under the *J* coupling, and this signal is recorded as a reference, S_0. The S_0 signal decays because of T_2 relaxation. If the two 45° pulses have

+x and −x phases to cancel each other, the *J*-coupling effects continue to accumulate and dephase the magnetization of $^{13}C-^{13}C$ spin-pairs. Spectrum *S* after J_{CC}-dephasing contains only signals of ^{13}C not bonded to another ^{13}C. The difference between S_0 and *S* is the spectrum of $^{13}C-^{13}C$ spin-pairs. The optimum duration of the J_{CC} modulation, 9.7 ms, was determined on a model compound, L-leucine-$^{13}C1,2$ (see Figure S2 of theSupporting Information). Because C1 and C2 are ^{13}C labeled, they show up in the S_0 spectrum (thin line) but are dephased by the C−C *J*-coupling in the *S* spectrum (thick line). The small peak at 27 ppm in both spectra is from the natural-abundance (isolated) methyl ^{13}C.

$^1H-^{15}N$ CP/MAS NMR. $^1H-^{15}N$ cross-polarization spectra were acquired with or without gated decoupling for dipolar dephasing, with a CP time of 2 ms at an MAS frequency of 5 kHz. The Hartmann−Hahn condition for cross-polarization was set carefully on the nonprotonated N of ^{15}N-t-BOC-L-proline. The 90° pulse length on the ^{15}N channel was 6 μs and the recycle delay, 3 s. TPPM decoupling was used during detection.

Selection of ^{15}N-Bonded Glycine-$^{13}C2$ and Glycine-$^{13}C2$-Bonded ^{15}N. To determine how many glycine C2's are bonded to ^{15}N, carbon-detected $^{13}C\{^{15}N\}$ REDOR experiments were applied to the glycine-$^{13}C2$-^{15}N labeled melanoidins. The total REDOR time was N t_r = 2 ms and the CP time was 1 ms at 5 kHz MAS. If the REDOR 180° pulses on the ^{15}N channel are turned off, the reference signal S_0 is obtained. With these REDOR 180° pulses switched on, the carbon signals are dephased by their adjacent nitrogen, and only the "*S*" signals of carbons not bonded to nitrogen remain. The intensity difference $\Delta S = S_0 - S$ is the spectrum of the carbons directly bonded to ^{15}N.

To determine what fraction of nitrogen remains in N−C2 bonds, nitrogen-detected $^{15}N\{^{13}C\}$ REDOR experiments were conducted at 5 kHz MAS. The pulse sequence and parameters are the same as in the corresponding $^{13}C\{^{15}N\}$ REDOR experiments, including the CP time of 1 ms, but with ^{15}N as the observed nucleus and REDOR pulses applied on the ^{13}C channel.

**Two-Dimensional $^{13}C-^{15}N$ HSQC.** To see the connectivity of glycine $^{13}C2$ with its ^{15}N after the Maillard reaction, 2D $^{13}C-^{15}N$ HSQC experiments, with CP time of 1 ms and REDOR recoupling for a total time of 1.14 ms, were performed at 7 kHz MAS.

Selection of ^{13}C Bonded to Nonprotonated ^{15}N. A $^{13}C-^{15}N$ REDOR period of 1.14 ms duration was used in this 1D experiment to transfer coherence between ^{13}C and ^{15}N (see Figure S3 of the Supporting Information). During the central period, the dipolar interactions between ^{15}N and ^1H can be recoupled for $2t_r$ (= 0.29 ms at 7 kHz MAS) of $^1H-^{15}N$ "REDOR". The S_0 signal was recorded without $^{15}N-^1H$ recoupling by simply continually applying decoupling pulses on the ^1H channel. The spectrum *S* is recorded after $^{15}N-^1H$ recoupling that dephases the coherence of protonated N. The CP contact time was 1 ms. Meanwhile, 40 μs gated decoupling between ^{13}C and ^1H before detection was also incorporated to selectively detect the signals of quaternary carbons. A short $^1H-^{13}C$ CP contact time of 50 μs with or without 40 μs of gated decoupling was applied to extract the protonated carbon signals.

The pulse sequences were tested on two model compounds. The first model compound, ^{15}N-t-BOC-L-proline, contains a nonprotonated N bonded to three carbons. Figure S4 of the Supporting Information shows that 75% of the reference signal in (a) remains after $2t_r$ = 0.29 ms of $^{15}N\{^1H\}$ dephasing in (b). Therefore, a scaling factor of 1/0.75 was used for the dephased melanoidin spectra below. The second model compound, ^{15}N-t-BOC-glycine-$^{13}C2$, contains a protonated N bonded to two carbons, of which one, a CH$_2$ carbon, is ^{13}C labeled. Because the nitrogen is protonated, only 8% of the full reference signal in Figure S4(c) remains in Figure S4(d) (Supporting Information).

RESULTS AND DISCUSSION

Transformations of Glucose and Glycine. The complexity of glucose transformations in the Maillard reaction is highlighted by the complex CP/MAS ^{13}C NMR spectra of unlabeled melanoidins formed in the dry and solution conditions, shown in **Figure 1a,b**, respectively (thin lines). Similarly complex spectra of melanoidins with signals ranging from 10 to 210 ppm have been reported before in the literature (*11, 15*). Spectra **c** and **d** of **Figure 1** shows selectively the signals of carbons originating from
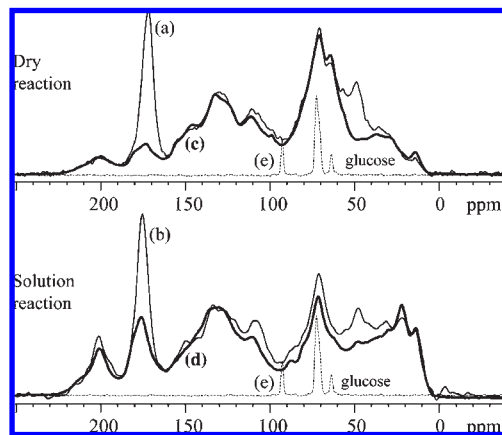
Figure 1. CP/TOSS ^{13}C NMR spectra of melanoidins made from glucose and glycine in a 1:1 molar ratio: (top panel) dry reaction; (bottom panel) solution reaction; (**a**, **b**) spectra of unlabeled samples (thin lines); (**c**, **d**) spectra of glucose-$^{13}C_6$ reacted with glycine-^{15}N (thick lines), scaled to match the broad features of the unlabeled samples; (**e**) spectrum of glucose for reference (dashed line), with the same line broadening as the other spectra.

glucose (thick lines), which were obtained by measuring melanoidins prepared from glucose-$^{13}C_6$ (and glycine-^{15}N). Dramatic transformations of glucose, from the simple three-line spectrum of neat glucose shown in **Figure 1e**, have clearly occurred during the Maillard reaction.

The differences in **Figure 1** between the spectra of all carbons and of those originating from glucose are mostly due to the carbons of glycine, which are seen to contribute mostly the sharp COO peak near 173 ppm and the N−$\underline{C}H_n$ signals near 50 ppm. This suggests that glycine carbons do not undergo changes as dramatic as those of glucose, especially in the dry reaction. This is confirmed in quantitative direct polarization ^{13}C NMR spectra of glycine carbons in melanoidins made from ^{13}C-labeled glycines, shown in **Figure 2**. The sharp peak of C1 (the COO carbon of glycine) at ~173 ppm is near its original position for neat glycine. The C2 carbon spectrum contains mostly bands in the alkyl region of the spectrum, with a dominant peak at ~50 ppm from untransformed NCH$_2$ moieties.

Extent of Glycine Loss. Differential degradation of reactants into volatile products during the Maillard reaction, as well as enrichment in low molecular weight fractions, can lead to loss of glycine relative to glucose in the high molecular weight melanoidins investigated here. This effect can be studied by quantifying the total ^{13}C NMR signals (see **Figure 2**) of glycine-$^{13}C1,2$, -$^{13}C1$, and -$^{13}C2$ in the melanoidins for the two reaction conditions. For reference, quantitative ^{13}C spectra of melanoidin made from glucose-$^{13}C_6$ reacted with ^{15}N-glycine in both dry and solution reaction have also been measured and integrated. They provide a basis for the calculation of glycine-C percentages with respect to all carbons. The total carbon of melanoidin is the sum of the integral of the glucose-$^{13}C_6$ signal and the integral of the glycine-$^{13}C1,2$ signal, normalized for the number of scans, receiver gain, and sample mass in the rotor and corrected for the signal of ^{13}C in natural abundance.

Given the 1:1 molar ratio of glucose and glycine reactants, the initial percentage of glycine carbon is 25% of the total reactant carbon. After the reaction, glycine carbon is found to contribute 24% of total carbon in the dry-reaction products and 22% in the solution-reaction products.

In both dry- and solution-reaction samples, ~42% (44% for the dry, 40% for the solution reaction) is from glycine C1 and the
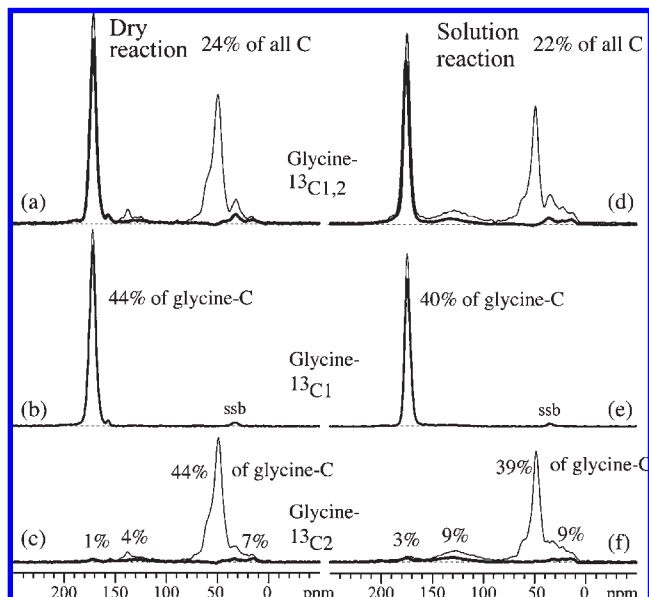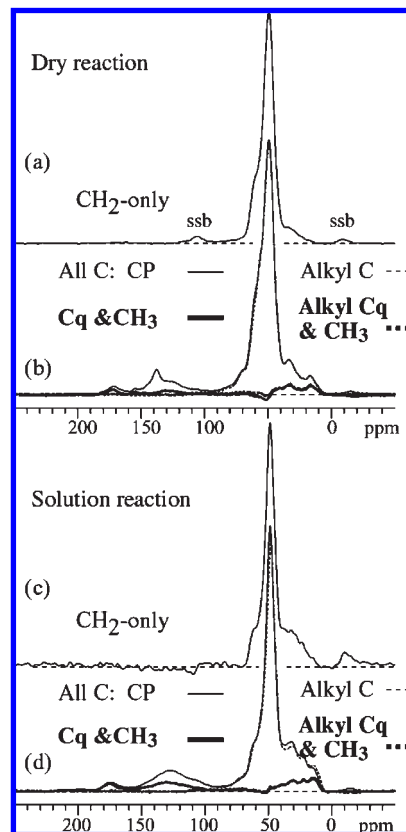
Figure 2. Quantitative direct polarization ^{13}C NMR spectra of melanoidins made from glucose reacted with various ^{13}C-labeled glycines: (thin lines) full spectra; (thick lines) corresponding selective spectra of quaternary carbons and methyl groups; (**a**−**c**) melanoidins from dry reaction; (**d**−**f**) melanoidins from solution reaction. The top two spectra are from melanoidins made from glycine-$^{13}C1,2$, accounting for 24 and 22%, respectively, of total carbons of the high molecular weight fraction. The middle row shows spectra of melanoidins made from glycine-$^{13}C1$, accounting for 44 and 40% of total glycine carbons, respectively. The bottom spectra are from samples made from glycine-$^{13}C2$, accounting for 56 and 60% of total glycine carbon, respectively. Most glycine C2 remains in its original NCH_2 structure, whereas smaller fractions formed COO moieties, aromatic carbon, and other alkyl types of carbons (the percentages of total glycine carbon are listed in the figure).

Figure 3. Selective ^{13}C NMR spectra of glycine-$^{13}C2$ labeled melanoidins from (**a**, **b**) the dry reaction and (**c**, **d**) the solution reaction: (**a**, **c**) CH_2-only spectra, obtained with three-spin coherence selection; (**b**, **d**) thick lines, full CP/TOSS spectra; thin lines, corresponding spectra of quaternary and methyl carbons, obtained after 40 μs of gated decoupling; dashed lines, corresponding selective spectra of all alkyl and of quaternary/CH_3 alkyl carbons.

remaining $\sim58\%$ from glycine C2. Thus, of the $\sim23\%$ of glycine carbons incorporated, $\sim0.42 \times 23\% = 10\%$ are C1 and $\sim0.58 \times 23\% = 13\%$ are C2. The difference of $\sim3\%$ of all carbons in the products can be attributed to loss of glycine C1 as CO_2 due to Strecker degradation and accounts for the slight reduction (~23 vs 25%) of glycine C in the products relative to the reactants.

Fate of Glycine C1. The quantitative ^{13}C spectra of the melanoidins prepared from glycine-$^{13}C1$ are particularly simple (see **Figure 2b,e**). The glycine-$^{13}C1$ melanoidin made in the dry reaction gives a single peak at 172 ppm, whereas the peak is at 174 ppm for the melanoidin made in solution, as in corresponding spectra of ref *22*. The slight intensity difference between the spectra without and with gated decoupling in **Figure 2b,e** arises from the ubiquitous two-bond $^{13}C-^{1}H$ dipolar couplings. The observed signals could be due to esters (COOC, 165−175 ppm), carboxylic acids (COOH, 170−180 ppm), carboxylates (COO⁻, 173−183 ppm), or amides (NC=O, 169−175 ppm). It should be noted that glycine C1 can form an amide only by reaction with the nitrogen from another glycine molecule; some such amides are detected below.

The ^{13}C CSA powder pattern can help us distinguish esters (COOC) from COOH or COO⁻, because the highest peak in the CSA powder pattern of esters is distinctly to the right of center, whereas that of COO⁻ is distinctly to the left and for COOH it is near the center of the spectrum (*29*, *32*). Figure S5 of the Supporting Information shows powder patterns, obtained using the SUPER technique (*29*), at various isotropic chemical shifts of glycine C1 in dry- and solution-reaction melanoidins. For the dry-reaction sample, the isotropic chemical shift of the peak

maximum is at 172 ppm, and the cross section shows the powder pattern resembling that of esters to a significant extent (see Figure S5(c) of the Supporting Information). For the solution-reaction sample with the main peak at 174 ppm, most powder patterns are similar to those of typical COOH groups.

Fate of Glycine C2; Absence of Enamines and Pyrazines. The fate of glycine-$^{13}C2$ can be assessed from the spectra in **Figure 2c,f**. After the Maillard reaction, the resonance near 50 ppm accounts for 44% of all glycine-C in dry-reaction melanoidin and 39% of all glycine-C in the solution-reaction sample. Dipolar dephasing and spectral editing techniques (see **Figure 3**) confirm that this is a CH_2 resonance; on the basis of the chemical shift, it can be assigned to NCH_2 carbons. This assignment is confirmed by carbon-detected $^{13}C\{^{15}N\}$ REDOR spectra of melanoidins prepared from glycine-$^{13}C2$-^{15}N, shown below.

It has been stated that "the C2 atom of amino acid is commonly incorporated into the polymer as an enamine-C" (*17*). Our spectra disprove that claim, which has always been speculative (*16*). If the enamine-C was part of a polymer chain, its double and single bonds to neighboring carbons allow bonding to at most one proton, that is, it could not be a CH_2 group, contrary to our experimental observations. A small signal of sp²-hybridized CH is observed near 130 ppm in **Figure 3**, but below, we show that this carbon is in fact not bonded to the putative enamine nitrogen resonating near 110 ppm (*16*). Furthermore, contrary to various enamine- or imine-based models of melanoidins (*14*, *17*, *18*), we also did not find the proposed protonated sp²-hybridized enamine or imine C bonded to 110-ppm N in our

Article

J. Agric. Food Chem., Vol. 57, No. 22, 2009   **10705**
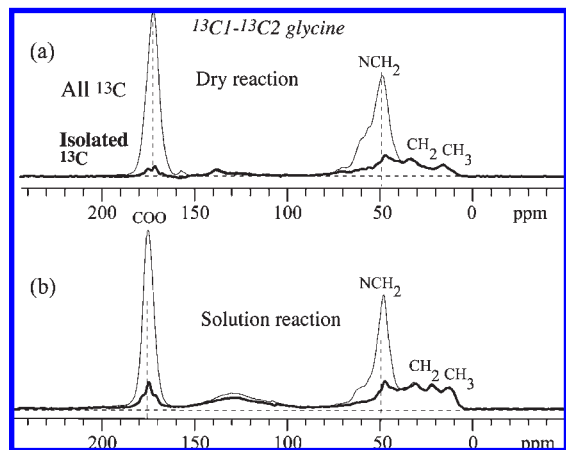
Figure 4. *J*-modulated spectra for glycine-[13]C1,2 labeled samples made (**a**) in the dry reaction and (**b**) in solution: (thin lines) reference spectra; (thick lines) isolated ^{13}C signals of degraded glycine. The difference intensity is from the glycine C1−C2 spin-pairs. For improved intensity of the minor signals, [1]H−[13]C cross-polarization was used for the spectra shown here. More quantitative but noisier *J*-modulated spectra after direct polarization have also been acquired and used in the quantitative analysis.

studies of melanoidins from glucose-[13]C1 and -[13]C6 (unpublished results).

Pyrazine ($C_4H_4N_2$) and pyridine rings are believed to be part of melanoidins because they have been detected at moderate concentrations in thermal degradation (*19, 20*). The four carbons of pyrazine would resonate at 146 ppm; other pyridinic carbons resonate around 150 ppm. The spectra of **Figures 2** and **3** do not show such a peak for our melanoidins. Below, we also show the lack of signals of pyrazine or pyridinic rings formed from glucose carbons.

Fate of the C1−C2 Bond of Glycine. The spectra in **Figures 2** and **3** show that some glycine C2 changed into various structures, for example, CCH_n, aromatic **NCH**, etc., whereas most of it remained in NCH_2 form. Are glycine C2 and C1 still chemically bonded with each other after these various reactions? If yes, there will be a 50 Hz *J*-coupling between the carbons; otherwise, the coupling will be negligible. The [13]C−[13]C *J*-dephasing pulse sequence of Figure S1 (Supporting Information) was applied to glycine-[13]C1,2 melanoidins to determine the extent to which the glycine C1−C2 bond has been broken. **Figure 4** displays the resulting spectra for the dry-reaction (**a**) and solution-reaction (**b**) samples. For recording the spectrum of all C, the homonuclear *J*-coupling evolution is refocused so that signals of all spin-pairs and isolated spins are observed (thin lines), whereas without the solid echo, the signals of carbon spin-pairs are dephased quickly via their *J*-coupling and only the spectrum of isolated carbons remains (thick lines in **Figure 4**).

The *J*-modulation results indicate that the C−C bond of most glycine molecules remains intact in the melanoidins. In the dry reaction, ∼78% of all glycine carbons are still bonded to each other and ∼65% in the solution-reaction sample. The isolated glycine C2 formed various species, such as aromatic **NCH**, C−CH_2−C CCH_3, NCH_3, and **COO** moieties. The broad background signal of isolated glucose ^{13}C in natural abundance is hardly visible in the spectra, but accounts for ∼5% of the total intensity and has been taken into account in the detailed quantification.

The data provide both the fraction of glycine C1 carbons remaining bonded to C2 carbons and the fraction of C2 remaining bonded to C1: According to *J*-dephasing, ∼95% of C1 carbons remain bonded to C2 after the dry reaction and ∼87%
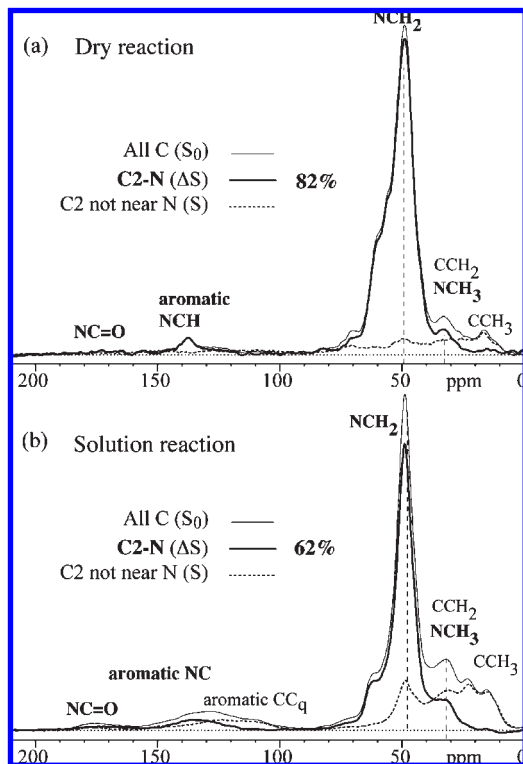
Figure 5. Carbon-detected [13]C{[15]N} REDOR spectra for glycine-[13]C2-^{15}N labeled melanoidins made in (**a**) dry and (**b**) solution reaction: (thin lines) reference spectrum S_0 of all carbons; (dashed lines) signal S of carbons at least two bonds from nitrogen, in degraded glycine; (thick lines) difference spectrum $\Delta S = S_0 - S$ of carbons directly bonded to nitrogen. The total REDOR time was $Nt_r = 2$ ms, at an MAS frequency of 5 kHz.

in solution. According to quantitative ^{13}C NMR, 44% of all glycine carbons are C1 after the dry reaction, so 0.95 × 44% = 42% of all glycine carbons are C1 bonded to C2 (35% in solution). Conversely, according to *J*-dephasing (with natural abundance and detection efficiency corrections), 64% of C2 carbons remain bonded to C1 in the dry reaction and 50% in solution. According to quantitative ^{13}C NMR, 56% of all glycine carbons are C2 after the dry reaction, so 0.56 × 64% = 36% of all glycine carbons are C2 bonded to C1 (30% in solution). The origin of the moderate discrepancy between the two calculations (42 vs 36%, 35 vs 30%) is not clear. Most of the data are from the same sample, we have ruled out incomplete T_1 or fast T_2 relaxation of the glycine-C2 signal in the DP spectra, and we have checked that the fraction of [13]C1−[13]C1 spin-pairs is negligible. Incomplete ^{13}C-labeling of the C2 site is a remote possibility. From the averages (in fact, sums) of the percentages for C1 and C2, we obtain values of 78 ± 6% C1−C2 after the dry reaction and 65 ± 5% C1−C2 after the solution reaction.

Fate of the C−N Bond of Glycine. The fraction of C−N bonds of glycine that remain intact can be determined from the intensities of [13]C{[15]N} REDOR spectra shown in **Figure 5**. When ^{13}C and ^{15}N are directly bonded, their dipolar coupling is >0.9 kHz, whereas two-bond couplings are >4 times smaller. Recoupling of the [13]C−[15]N dipolar interaction via REDOR of $Nt_r = 2$ ms duration dephases the signals of carbon bonded to ^{15}N, and only the signals of carbons not bonded to N are recorded in the spectrum S (dashed thin lines in **Figure 5**). Without the REDOR pulses, signals of all types of carbons are recorded in a reference spectrum S_0 (thin lines in **Figure 5**). Therefore, the difference $\Delta S = S_0 - S$ (thick lines) is the spectrum of the ^{13}C directly bonded to [15]N. Taking the full integral of the ΔS spectrum
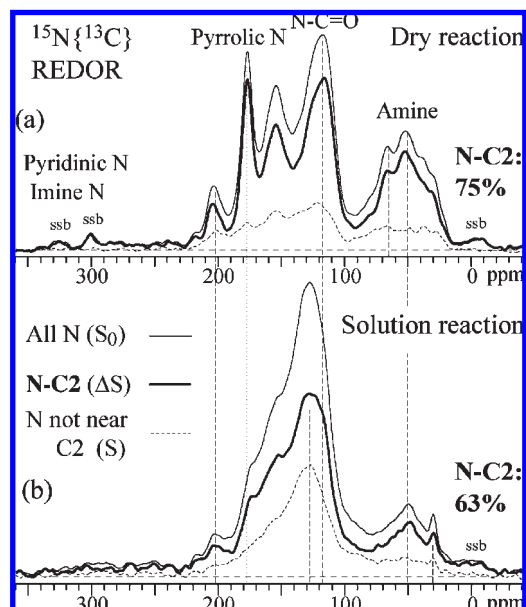
**Figure 6.** Nitrogen-15 detected $^{15}N\{^{13}C\}$ REDOR spectra of glycine-$^{13}C2$-^{15}N labeled melanoidins from (**a**) dry and (**b**) solution reaction: (thin line) reference spectrum S_0 without C−N recoupling; (dashed thin line) spectrum S of nitrogen far from glycine-C2, from degraded glycine; (thick line) difference spectra $\Delta S = S_0 - S$ of nitrogen directly bonded to glycine-C2 (75% of nitrogen in dry reaction and 63% of nitrogen in solution reaction). Spinning frequency = 5 kHz; CP time = 1 ms. Spinning sidebands are labeled "ssb".

relative to that of S_0 shows that ∼82 or 62% of glycine C2 in the dry- or solution-reaction samples, respectively, remains bonded to N. In the dry reaction, more glycine C2 remains in NCH$_2$ moieties.

The spectra also confirm the assignments of the glycine $^{13}C2$ resonances in melanoidins. The ΔS spectra in **Figure 5** show the highest peaks at 50 ppm for both samples, proving that these dominant peaks in **Figure 2c,f** are NCH$_2$. In addition, there are signals of NCH$_3$ (at 35 ppm) and N-bonded aromatic carbon (around 135 ppm) in the ΔS spectrum, and CCH$_n$ signals (from 40 to 10 ppm) in the S spectrum. It is interesting to note that signals of O−CH, O−CH$_2$, and C=O groups, which might be expected from the incorporation of the aldehyde formed by C2 in Strecker degradation, are only minimally present, as witnessed by minimal signals in the N-dephased ^{13}C spectrum S (dashed line in **Figure 5**) near 75, 65, or 185 ppm.

Furthermore, by switching the detected nucleus to ^{15}N we can probe the breaking of C−N bonds from a different perspective. $^{15}N\{^{13}C\}$ REDOR spectra measured for this purpose are plotted in **Figure 6**, panels **a** and **b**, for glycine-$^{13}C2$-^{15}N labeled melanoidins made in the dry and solution reaction, respectively. Here, we focus on the effect of $^{13}C2$ on the overall ^{15}N intensities; the spectral features will be discussed below. The difference spectra (thick lines) between S_0 (thin lines) and S (dashed thin lines) represent the nitrogen directly bonded to glycine-$^{13}C2$. According to **Figure 6**, 75 and 63% of nitrogen are bonded to glycine-C2 made in dry and solution reactions, respectively.

Comparison of the fractional intensities of the $^{13}C\{^{15}N\}$ and $^{15}N\{^{13}C\}$ ΔS REDOR spectra shows that there is no large percentage difference for the solution-reaction sample: 62% of glycine-C2 is directly bonded to nitrogen, and 63% of nitrogen is directly bonded to glycine-C2. However, for the dry-reaction sample, 82% of glycine C2 stays bonded to nitrogen, whereas slightly less, 75%, of nitrogen remains bonded to glycine C2.
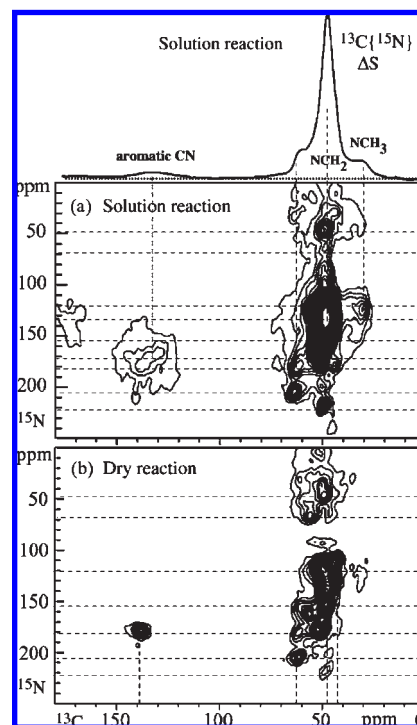
Figure 7. 2D $^{15}N-^{13}C$ HSQC spectra for glycine-$^{13}C2$-^{15}N labeled melanoidins made in (**a**) solution and (**b**) dry reaction, acquired at an MAS frequency of 7 kHz. The one-dimensional spectrum of C2 bonded to N for the solution reaction, obtained by $^{13}C\{^{15}N\}$ REDOR difference, is shown at the top of the figure.

The difference suggests that slightly more nitrogen remains in the dry-reaction melanoidin or that several glycine-C2's simultaneously bond to the same nitrogen, which is possible for the aromatic C2H bonded to NC2H$_2$, because they show two cross peaks in **Figure 7b** at the same imidazolium nitrogen chemical shift position around 180 ppm; this hypothesis is confirmed below by $^{15}N\{^{13}C\}$ dephasing in melanoidins made from glucose-$^{13}C_6$ and glycine-^{15}N.

Fate of Glycine N. The transformation of glycine nitrogen in the melanoidins can be assessed from the ^{15}N NMR spectra, such as the S_0 spectra shown in **Figure 6**. Whereas the ^{13}C spectra of each of the glycine carbons shown above are quite simple, the nitrogen spectra show many bands over a wide range of chemical shifts, comparable to the many ^{13}C bands of glucose carbons in **Figure 1**. For ^{15}N-labeled melanoidins made by solution reaction, Benzing-Purdie et al. (*10*) and Hayase et al. (*16*) observed spectra similar to that in **Figure 6b**, although significantly noisier. Two major ranges of ^{15}N resonances can be distinguished: sp^3-hybridized (amine) N between 80 and 0 ppm and sp^2-hybridized N resonating from 80 to 215 ppm, including amide N resonating at ∼120 ppm, pyrrole N (∼150 ppm), imidazolium N (∼170 ppm), and oxazolium N (∼200 ppm). These assignments will be justified in a future publication, based on $^{15}N-^{13}C-^{13}C$ NMR experiments.

This composition is not properly reflected in thermal degradation analyses of melanoidins (*19, 20*), which often feature little amine or imidazolium nitrogen, but instead some pyridine and pyrazine. We find that all types of pyrrolic N accounts for < 40% of all N in both types of melanoidins studied (N in regular pyrrole rings resonating near 150 ppm for even less, < 20%), with amide and amine N accounting together for more than half of N. Although Hayase et al. questioned the presence of pyrrole in melanoidin, their spectra are actually fully consistent with the

Article

J. Agric. Food Chem., Vol. 57, No. 22, 2009   **10707**

Table 1. Approximate Amounts of the Forms of Nitrogen in the Two Melanoidins Studied, as a Percentage of Total Glycine Nitrogen

| sample	aromatic N (pyrrolic) (%)	amide (NC=O) (%)	amine (%)	N—H (%)	nonprotein N_t (%)
dry	39	33	28	21 ± 2	79 ± 2
solution	31	53	16	15 ± 5	85 ± 5

presence of pyrrole and furan rings and their quite selective removal by ozone (*16*). Iminium (C=N$^+$<) signals overlap with those of pyrrolic N and cannot be excluded on the basis of our ^{15}N NMR spectra. However, no significant ^{15}N NMR signals of pyridines or pyrazines (between 250 and 350 ppm) or of imines (C=N—C, between 300 and 370 ppm) are observed in our or any published spectra (*10*, *16*). The absence of six-membered heterocyclic rings will be further discussed below in the context of the ^{13}C{^{15}N} spectra of **Figure 10**.

The samples from dry and solution reactions show somewhat different ^{15}N spectral features. For the solution reaction, most nitrogen is in amides, whereas the dry reaction distributes nitrogen more evenly among amine, amide, pyrrole, imidazolium, and oxazolium nitrogen (see **Table 1**). It is interesting to note that although the amide signal dominates the ^{15}N spectrum, it corresponds only to a minor peak ($< 0.5 \times 1/8 = 6\%$ of the total area) in the ^{13}C spectrum (peaks near 172 ppm in the thick-line spectra of **Figure 1**), given the N:C ratio of 1:8 in the reactants. Neither sample shows strong ^{15}N NMR intensity beyond 220 ppm, excluding a major contribution from pyridinic nitrogen.

After dephasing of the ^{15}N signal by ^{13}C2 of glycine, the spectrum *S* of the molecules fragmented at the C2—N bond, as in Strecker degradation, is obtained. It is shown dashed in **Figure 6**. In terms of relative signal intensities, this spectrum of the fragmented molecules does not differ significantly from the ΔS spectrum without Strecker degradation, indicating that Strecker degradation does not change the incorporation of N dramatically.

Whereas most of the intensity of the ^{13}C2{^{15}N}REDOR ΔS spectra in **Figure 5** resides in a single NCH$_2$ band, in the two-dimensional ^{13}C—^{15}N HSQC spectra displayed in **Figure 7** this main peak is dispersed widely along the vertical ^{15}N dimension, for both reaction conditions. The 2D spectrum resolves a dozen or more bands, many more than observed in the 1D ^{15}N spectrum. All of those different forms of nitrogens are bonded to CH$_2$ of glycine C2, which indicates that nitrogen is an active site for reactions incorporating glycine into melanoidins, but usually without breaking the bond to glycine C2. According to the 2D HSQC spectrum, a relatively small fraction of aromatic C2H resonating at 132—138 ppm is bonded to imidazolium nitrogen for both reaction conditions. It is not bonded to putative enamine nitrogen resonating near 110 ppm (see discussion above). Also, some glycine C2 in NCH$_3$ groups, resonating at 30 ppm, is seen to be bonded to amide (N—C=O) nitrogen; ^{15}N{^{1}H} dipolar dephasing (data not shown) proves that these amides are mostly not protonated.

Insights into the Fate of Glycine by Difference. Information on the fate of glycine N and C can also be gleaned from studies of samples made from glycine-^{15}N and glucose-^{13}C$_6$. Again based on the strongly distance-dependent ^{15}N—^{13}C dipolar coupling, we can select the signal of nitrogens that are not near glucose ^{13}C and which must therefore be bonded exclusively to glycine carbons. **Figure 8** shows ^{15}N{^{13}C}REDOR reference (S_0) and dephased (*S*) spectra; the latter contain only signals of nitrogen not bonded to ^{13}C, that is, not bonded to glucose. The *S'* spectrum after N—H dipolar dephasing is also shown, allowing us to determine whether these are nonprotonated N.
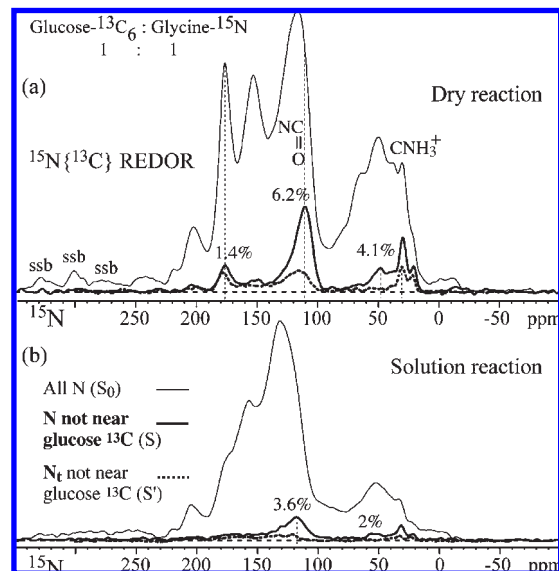
Figure 8. Nitrogen-15 detected ^{15}N{^{13}C} REDOR spectra of melanoidins made from glycine-^{15}N and glucose-^{13}C$_6$: (**a**) dry reaction; (**b**) solution reaction; (thin lines) reference spectrum (S_0) without C—N recoupling: (thick full line) ^{13}C-dephased spectrum (*S*) of nitrogen not bonded to glucose carbons (i.e., bonded only to glycine C); (thick dashed line) ^{13}C-dephased spectrum (*S'*) with additional recoupled N—H dipolar dephasing, showing only signals of nonprotonated N not bonded to glucose C. Spinning frequency = 5 kHz; CP time = 1 ms.

Two distinct bands are observed in spectrum *S* after dephasing. A peak of mostly nonprotonated N observed at ~180 ppm confirms that imidazolium-N bonded to three glycine carbons (which must be C2 because C1 does not form aromatic rings) is present at a level of 1.4% of all N in the dry-reaction melanoidin, as proposed above on the basis of the 7% difference between glycine C2—N and N—C2 bonding fractions. In the sample made in solution, where no C2—N/N—C2 difference was found, the corresponding signal near 180 ppm is significantly smaller. A peak at 110 ppm, accounting for 6.2% of all N, two-thirds of which are protonated, can be assigned to amide (NC=O) nitrogen. Given that an amide nitrogen must be bonded to a C=O carbon, and the carbon is not from glucose, this shows that ~6% of glycine carbons form peptide bonds (H—N—C=O) or O=C—NH$_2$ end groups. The chemical shift of 110 ppm matches that of N in glycyl residues in polypeptides, indicating that these C—N—(C=O) units, with all atoms from glycine, could be part of glycyl dimer units. Because this exceeds the ~1.5% fraction of C2=O carbons (see **Figure 2**), it must contain a ~5% contribution of NC1=O. Thus, in addition to the dominant COO forms of C1 discussed above, formation of some NC1=O amides has been indirectly detected.

(Non)protonation of Nitrogen. Whereas the carbons of glycine undergo relatively little transformation, its nitrogen is incorporated into a wide range of different structures formed by glucose carbons. Whether nitrogen remains bonded to H or not can be assessed by ^{1}H—^{15}N dipolar dephasing experiments, where ^{1}H dipolar decoupling is switched off to allow the ^{1}H nuclear magnets to destroy the magnetization of nearby (i.e., directly bonded) ^{15}N spins. CP/MAS ^{15}N NMR spectra with optimized cross-polarization and with or without recoupled dipolar dephasing are shown in **Figure 9** for the dry-reaction (**a**) and solution-reaction (**b**) melanoidins. The spectra after dipolar dephasing (thick lines) in **Figure 9** show that a large fraction (> 75%) of the nitrogen is not protonated. In particular, > 90% of pyrrole N is
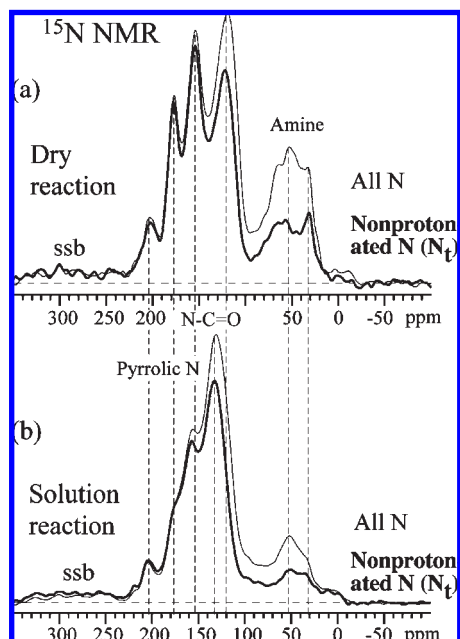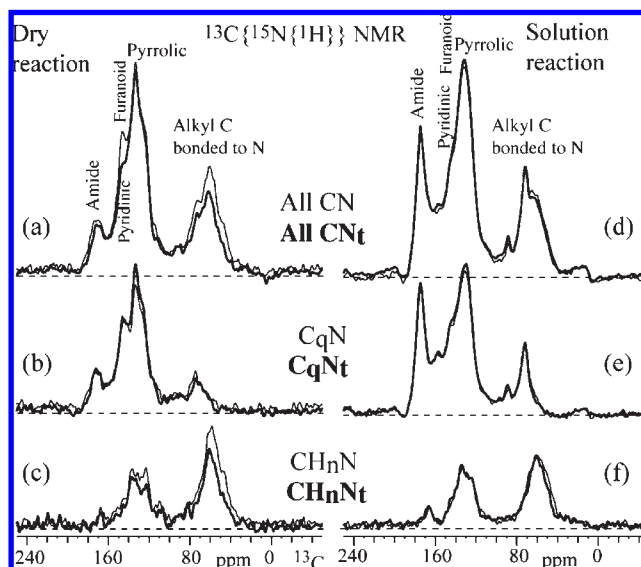
Figure 9. $^1H-^{15}N$ CP spectra of glycine-^{15}N labeled melanoidins from (**a**) dry reaction of glucose-$^{13}C1$ and glycine-^{15}N and (**b**) solution reaction of glucose-$^{13}C_6$ and glycine-^{15}N: (thin line) spectrum of all nitrogen; (thick line) spectrum of nonprotonated nitrogen, selected by two rotation periods of recoupled $^1H-^{15}N$ dephasing before detection and scaled up by a factor of 1/0.61 determined on ^{15}N-t-BOC-L-proline. Spinning frequency = 5 kHz, contact time = 2 ms. Spinning sidebands are marked by "ssb".

Figure 10. Carbon-detected 1D $^{13}C\{^{15}N\{^1H\}\}$-HSQC-REDOR NMR of melanoidins made in the dry and solution conditions from glucose-$^{13}C_6$ reacting with glycine-^{15}N: (left) dry reaction; (right) solution reaction; (thin lines) reference REDOR difference spectra of carbons bonded to both protonated and nonprotonated nitrogen, after Nt_r = 1.14 ms of $^{13}C\{^{15}N\}$ recoupling; (thick lines) corresponding spectra of carbons bonded to nonprotonated nitrogen, selected by 0.29 ms $^{15}N\{^1H\}$ dephasing and scaled up by the factor of 1/0.75 determined in a model compound (see Figure S4(b) of the Supporting Information). (**a**) and (**d**) are spectra of all types of carbon near N, (**b**) and (**e**) are from nonprotonated carbons, and (**c**) and (**f**) are from protonated carbons. The spectra show that nitrogen in melanoidins is predominantly not protonated.

not protonated, whereas thermal degradation studies have reported various pyrroles with N—H groups (*19, 20*). Amide groups are predominantly not of the secondary —C—NH—C=O type found in peptides and proteins, but mostly tertiary, with N bonded to three carbons.

In ^{15}N NMR experiments with cross-polarization from ^1H, signals of nonprotonated nitrogens are underrepresented. Due to the lower gyromagnetic ratio of nitrogen, transfer of polarization from protons to nonprotonated N takes ~2.5 times longer than for nonprotonated carbons and is more susceptible to averaging by moderate-speed MAS. Within the typical cross-polarization times of 1−2 ms, protonated nitrogen with its 10 kHz $^1H-^{15}N$ coupling will get more magnetization from protons. To avoid the differential enhancement of protonated N, we have developed a method of probing the protonation of ^{15}N with ^{13}C detection, using $^{13}C\{^{15}N\{^1H\}\}$-HSQC-REDOR. As shown in Figure S3 of the Supporting Information, $^{15}N-^1H$ "REDOR" is embedded within a $^{13}C-^{15}N-^{13}C$ coherence transfer sequence analogous to $^{15}N-^{13}C$ HSQC NMR. During the central period with transverse ^{15}N and longitudinal ^{13}C coherence, $^{15}N-^1H$ recoupling is turned on for two rotation periods to dephase the nitrogen bonded to ^1H; then, the detected ^{13}C must be near nonprotonated ^{15}N (thick lines in **Figure 10**). Without $^{15}N-^1H$ recoupling, the detected ^{13}C is near all types of ^{15}N (thin lines in **Figure 10**). In addition, gated decoupling before ^{13}C detection and a short CP contact time can be applied to spectrally edit nonprotonated and protonated ^{13}C.

The spectra in **Figure 10** are from melanoidins made from glucose-$^{13}C_6$ reacted with glycine-^{15}N in dry (**a**−**c**) and solution conditions (**d**−**f**). The thin-line spectra are for the carbons near all types of nitrogen and the thick-line spectra for carbon near nonprotonated nitrogen, scaled by the factor of 1/0.75 determined in model compounds. Spectra shown in **Figure 10a**,**d** are for all types of carbons, those in **Figure 10b**,**e** for nonprotonated carbons, and those in **Figure 10c**,**f** for protonated carbons. The

figure shows that nitrogen is predominantly not protonated regardless of whether the nearby carbon is protonated or not. In the analysis of the intensities, it needs to be taken into account that a tertiary N is bonded to two glucose ^{13}C, whereas N−H is bonded to only one such ^{13}C. Spectral integrals taking these factors into account give N_t:NH ratios of 79:21 and 92:8 for the melanoidin from dry and solution reaction, respectively. Quite similar values were found in the same experiment for the glycine-$^{13}C2$ labeled samples (not shown). With ^{15}N detection, an (underestimated) 75:25 ratio is obtained for both samples. Values averaged between ^{15}N- and ^{13}C-detected results are given in **Table 1**. The large fraction of nonprotonated N in melanoidins represents a clear distinction from peptides and amino sugars, where most N is protonated, and can thus be a useful marker of Maillard reaction products, for instance, in natural organic matter.

For 1:1 glucose/glycine ^{15}N-labeled melanoidins made in solution, Benzing-Purdie et al. (*10*) observed spectra similar to that in **Figure 9b**, but they assigned the main peak to secondary (H—N—C=O) rather than tertiary amides; due to noise, they also failed to recognize the additional peaks downfield from the main band, which are more pronounced in the dry-reaction sample and can be assigned to imidazolium and oxazolium rings.

Pyrazine and Other Pyridinic Rings. The spectra of glucose ^{13}C bonded to ^{15}N in **Figure 10** can also provide information on the types of nitrogen-containing moieties in the melanoidins. The ^{15}N spectra of **Figure 6** did not exhibit signals of pyrazine or other six-membered heterocyclic rings. The insignificance of pyridine contributions is confirmed by the ^{13}C spectra of **Figure 1**, which do not show a strong signal characteristic of pyrazine rings at 146 ppm or more generally of pyridinic C near 150 ppm. This is corroborated by $^{13}C\{^{15}N\}$ NMR spectra of melanoidins made from glucose-$^{13}C_6$ and glycine-^{15}N in **Figure 10**, which selectively

Article

J. Agric. Food Chem., Vol. 57, No. 22, 2009 **10709**

exhibit signals of ^{13}C bonded to ^{15}N. In these spectra, the potential signal of pyridinic C near 150 ppm is quite small compared to that of amide, pyrrolic, and amine moieties. Interestingly, the $^1H-^{15}N$ dephasing of the peak at 146 ppm in **Figure 10a**, thin line versus thick line, shows that at least part of the signal is *not* from pyrazine, the nitrogen of which is not protonated. Instead, these signals may be from aromatic carbons bonded to both N and O (e.g., in oxazole-related structures). Furthermore, the limited $^1H-^{13}C$ dipolar dephasing of the signal near 150 ppm in the spectra of **Figure 10b,e** show that most pyridinic carbons would have to be not protonated, unlike the structures seen in thermal degradation (*19*).

Structural Units of Glycine in Melanoidins. Evaluation of the various ^{13}C, ^1H, and ^{15}N solid-state NMR spectra of melanoidins made from suitably ^{13}C- and ^{15}N-labeled glycine reveals that several structural units containing glycine C2 can be identified and quantified, as listed in **Table 2**. Glycine C1 remains mostly in its COO environment. To determine their percentages, spectral bands in the various spectra have been integrated. Some bands cannot be resolved in the quantitative ^{13}C spectra, as seen in

Figure 2c,f. ^{13}C detected $^{13}C\{^{15}N\}$ REDOR experiments are useful to separate NCH_2, NCH_3, CCH_2, CCH_3, N-aromatic carbon, and non-nitrogen aromatic carbon resonances. A signal near 50 ppm of C not dephased by N is tentatively assigned to CCH groups (methines bonded to three carbons). Because the $^{13}C\{^{15}N\}$ REDOR experiments did not use direct polarization of ^{13}C, the relative peak intensities are not fully quantitative. Therefore, we first integrated several regions in the $^{13}C\{^{15}N\}$ REDOR spectra as shown in **Figure 5**, to obtain S/S_0 ratios for each spectral range. Correct S_0 intensities were obtained from the area fractions of the corresponding bands in the quantitative ^{13}C NMR data listed in **Figure 2c,f**. Data from the *J*-dephased spectra were treated accordingly.

Quantification of Glycine Fragmentation. To quantify the breakup of glycine in the Maillard reaction, we first need to convert from the fractions of glycine in the product to fractions of glycine reactant. We have found that 56% of glycine C in the product after dry reaction is from glycine-C2, which corresponds to 50% of C in the relevant glycine reactant. Thus, the glycine *reactant* contained 1.12 times more carbon than the glycine C *in the melanoidin* after the dry reaction. Correspondingly for the solution reaction, 60% of glycine C in the products is from glycine-C2; thus, the correction factor is 1.2. Given the 12% "excess" of reactant C2, compared to C1, remaining after the dry reaction, C1 must have been lost as CO_2 for $2 \times 12\%/1.12 = 21\%$ of all glycine reactant; this CO_2 loss is characteristic of Strecker degradation. In solution, for $2 \times 20\%/1.2 = 33\%$ of glycine reactant, C1 was lost as CO_2.

Quantitative analysis of J_{CC}-dephasing of the C1 resonance shows that $2 \times 3\%/1.12 = 5\%$ of all glycine fragmented without loss of C1 in the dry reaction and $2 \times 7\%/1.2 = 12\%$ in solution. Half of these glycine carbons (3 and 6%, respectively) are isolated C1 (see **Tables 3** and **4**), whereas the other half contribute to "isolated C2" or "other C2−N". As discussed above, J_{CC}-dephasing also yielded estimates of the fraction of glycine C1−C2 bonds in the melanoidin. Glycine C1−C2 pairs account for $78\%/1.12 = 70\%$ of all glycine reactant after the dry reaction and for $65\%/1.2 = 54\%$ after the solution reaction. These values

Table 2. Structural Units into which Glycine C2 (in Bold; with C1 in Italics and Underlined) Has Been Transformed during the Maillard Reaction and Their Percentages of Total Glycine Carbon in the Melanoidins[a]

N-**CH₂**-*COO* (C2 *C1*)	Other N-**CH₂**	O‖ *C*-N**CH₃**	C**CH₂**C	C**CH₃**	*C*CH[†]
Dry	**33%**	8%	3%	3%	2%	*1.2%*
Sol.	**25%**	9%	3%	5%	2%	*4%*

	C-*COO*	N⟩**N-CH₂** ⟨*C*	⟩N− ⟨*C* Other aromatic **C**	**COO**	Total **C2**
Dry	2%	**1.4** +*1.4%*	**0%**	0%	1%	56%
Sol.	3%	**0.7** + *0.7%*	**3.5%**	1%	3%	60%

[a] Percentages of N−C moieties from glycine are in bold; those of C1−C2 moieties are in italics. Thus, values for N−C1−C2 moieties are in bold italics. Error margins: ±2%. [†] Uncertain assignment.

Table 3. Fractions of C in Glycine Reactants Incorporated into Melanoidin after Dry Reaction or Lost as CO_2[a]

	C1-C2		C2-N				Total
	70±5%		75±4%				
Isolated C1	Other C1-C2	C1-C2-N	Other C2-N	Isolated C2	C1 lost	
3%	6%	59±4%	11%	7%	15%	101%
Other degradation		No degr.	Other	Strecker degradation		
9%		59±4%	3%	27±4%		99%

[a] "Other C1−C2" refers to C1−C2 pairs that are not bonded to N (deamination products), "other C2−N" to C2−N fragments not bonded to C1 (decarboxylation products), "isolated C2" to C2 bonded to neither C1 nor N, and "other" or "other degradation" to degradation which, unlike Strecker degradation, does not involve loss of C1. The sums of the percentages within the two full rows are compatible with 100% within the error margins, while the sum of the first row exceeds 100% because the same C2 carbon (in C1−C2−N moieties) can contribute to both categories.

Table 4. Fractions of C in Glycine Reactants Incorporated into Melanoidin after Solution Reaction or Lost as CO_2[a]

	C1-C2		C2-N				Total
	54±4%		62±3%				
Isolated C1	Other C1-C2	C1-C2-N	Other C2-N	Isolated C2	C1 lost	
6%	12%	42±4%	14%	10%	17%	101%
Other degradation		No degr.	Other	Strecker degradation		
18%		42±4%	6%	33±4%		99%

[a] Percentages within the two full rows add up to 100% within the error margins. The terminology is the same as in **Table 3**.

10710 *J. Agric. Food Chem.,* Vol. 57, No. 22, 2009

Fang and Schmidt-Rohr

are listed in **Tables 3** and **4**. The fractions of C2−N bonds, which were determined above and are also given in the first row of either table, do not need to be corrected for loss of C1, because C1 is not involved in the C2 and N statistics. The sum of the entries in the first rows of **Tables 3** and **4** exceeds 100% because C1−C2−N segments contain both a C1−C2 and a C2−N fragment, and the C2 carbon is thus counted twice.

In the center of the next row of **Tables 3** and **4**, the fraction of unfragmented glycine molecules (C1−C2−N) is given. It has been obtained from the first entry in **Table 2**, after multiplication by 2 to account for both C2 and C1 and correction for C1 loss. Thus, it is 2 × 33%/1.12 = 59% for dry reaction and 2 × 25%/1.2 = 42% for solution reaction. According to **Table 2**, (8% + 3% + 1.4%)/1.12 = 11% of C2−N segments not bonded to C1 are produced in the dry reaction (14% in solution), partly by Strecker degradation and partly (2 × 3% in dry, 2 × 6% in solution reaction, see above) by other fragmentation of the C−C bond without loss of C1. Note that C1 or C2 without the other carbon bonded is counted only half.

Also according to **Table 2**, there are 2(1.2% + 2%)/1.12 = 5.7% of C1−C2 fragments not bonded to N after dry reaction (12% in solution). Further listed in the second rows of percentages in **Tables 3** and **4** are isolated C2 without bonds to C1 or the "original" N (from entries in **Table 2** that are neither bold nor italic), which account for (3% + 2% + 1.4% + 1%)/1.12 = 6.6% of glycine carbons in dry reaction (10% in solution). The fraction of lost C1 is the difference between the fractions of C2 not bonded to C1 (from entries in **Table 2** that are not bold) and the isolated C1, 18% − 2% = 16% (23% in solution). Alternatively, based on 21% of Strecker degradation, it is 21%/2 = 11% for the dry reaction (17% in solution). This comparison suggests that 21% underestimates the extent of Strecker degradation in the dry reaction and that 27 ± 4% is a better estimate. On the basis of these calculations, good estimates of the fractions of the various glycine fragments have been obtained, as summarized in **Table 3** for the dry reaction and in **Table 4** for the solution reaction. By comparison, in a previous NMR study Strecker degradation was significantly overestimated because all types of fragmentation, including deamination, were attributed to this pathway, even if C1 remained in the melanoidin (*22*).

In conclusion, most glycine is stoichiometrically incorporated into the products, and the main fraction of glycine molecules remains intact (59% in dry reaction, 42% in solution reaction). Strecker degradation breaks up about one-fourth of glycine in the dry reaction and about one-third in solution reaction. Other degradation reactions without loss of C1 affect about one-eighth of all glycine in the dry reaction and about one-fourth in solution. The C1 carbon remains mostly in a COO group, whereas the nitrogen is incorporated into a wide variety of amide, amine, and pyrrolic species, but not enamines, imines, or pyrazines. Nonprotonated N predominates (>78%) and may be a characteristic marker of Maillard reaction products, for instance, in natural organic matter, distinguishing them from proteinaceous materials and amino sugars, where most nitrogen is in NH groups.

Supporting Information Available: Figures S1−S5. This material is available free of charge via the Internet at http://pubs.acs.org.

LITERATURE CITED

(1) Hodge, J. E. Chemistry of browning reaction in model system. *J. Agric. Food Chem.* **1953**, *1*, 926–943.

(2) Ledl, F.; Schleicher, E. New aspects of the Maillard reaction in foods and in the human body. *Angew. Chem. Int. Engl. Ed.* **1990**, *29*, 565–594.

(3) Tressl, R.; Kersten, E.; Rewicki, D. Formation of pyrroles, 2-pyrrolidones, and pyridones by heating of 4-aminobutyric acid and reducing sugars. *J. Agric. Food Chem.* **1993**, *41*, 2125–2130.

(4) Tressl, R.; Wondrak, G. T.; Garbe, L. A. Pentoses and hexoses as sources of new melanoidin-like Maillard polymers. *J. Agric. Food Chem.* **1998**, *46*, 1765–1776.

(5) Nursten, H. *The Maillard Reaction: Chemistry, Biochemistry and Implications.* Royal Society of Chemistry, London, **2005**.

(6) O'Brien, J.; Nursten, H. E.; Crabbe, M. J.; Ames, J. M. *The Maillard Reaction in Foods and Medicine*; RSC Publishing: Cambridge, U.K., 1998.

(7) Tessier, F.; Obrenovich, M.; Monniers, V. M. Structure and mechanism of formation of human lens fluorophore LM-1. *J. Biol. Chem.* **1999**, *274*, 20796–20804.

(8) Chellan, P.; Nagaraj, R. H. Protein crosslinking by the Maillard reaction: dicarbonyl-derived imidazolium crosslinks in aging and diabetes. *Arch. Biochem. Biophys.* **1999**, *368*, 98–104.

(9) Hoering, R. C. A comparison of melanoidins and humic acid. *Carnegie Inst. Washington Yearb.* **1973**, *72*, 682–690.

(10) Benzing-Purdie, L.; Ripmeester, J. A.; Preston, C. M. Elucidation of the nitrogen forms in melanoidins and humic acid by nitrogen-15 cross polarization-magic angle spinning nuclear magnetic resonance spectroscopy. *J. Agric. Food Chem.* **1983**, *31*, 913–915.

(11) Ikan, R.; Ioselis, P.; Rubinsztain, Y.; Aizenshtat, Z.; Pugmire, R.; Anderson, L. L.; Woolfenden, W. R. Carbon-13 cross polarized magic angle samples spinning nuclear magnetic resonance of melanoidins. *Org. Geochem.* **1986**, *9*, 199–212.

(12) Stevenson, F. J. Humus chemistry: genesis, composition. *Reactions.* Wiley: New York, 1994.

(13) Vandebroucke, M.; Largeau, C. Kerogen origin, evolution and structure. *Org. Geochem.* **2007**, *38*, 719–833.

(14) Kato, H.; Tsuchida, H. Estimation of melanoidin structure by pyrolysis and oxidation. *Prog. Food Nutr. Sci.* **1981**, *5*, 147–156.

(15) Benzing-Purdie, L.; Ripmeester, J. A.; Ratcliffe, C. I. Effects of temperature on Maillard reaction products. *J. Agric. Food Chem.* **1985**, *33*, 31–33.

(16) Hayase, F.; Kim, S. B.; Kato, H. Analyses of the chemical structures of melanoidins by ^{13}C NMR, ^{13}C and ^{15}N CP-MAS NMR spectrometry. *Agric. Biol. Chem.* **1986**, *50*, 1951–1957.

(17) Cämmerer, B.; Kroh, L. W. Investigation of the influence of reaction conditions on the elementary composition of melanoidins. *Food Chem.* **1995**, *53*, 55–59.

(18) Yaylayan, V. A.; Kaminsky, E. Isolation and structural analysis of Maillard polymers: caramel and melanoidin formation in glycine/glucose model system. *Food Chem.* **1998**, *63*, 25–31.

(19) Adams, A.; Tehrani, K. A.; Keršienė, M.; Venskutonis, R.; De Kimpe, N. Characterization of model melanoidins by the thermal degradation profile. *J. Agric. Food Chem.* **2003**, *51*, 4338–4343.

(20) Tehrani, K. A.; Keršienė, M.; Adams, A.; Venskutonis, R.; De Kimpe, N. Thermal degradation studies of glucose/glycine melanoidins. *J. Agric. Food Chem.* **2002**, *50*, 4062–4068.

(21) Wedzicha, B. L.; Kaputo, M. T. Melanoidins from glucose and glycine: composition, characteristics and reactivity towards sulphite ion. *Food Chem.* **1992**, *43*, 359–367.

(22) Benzing-Purdie, L.; Ripmeester, J. A. Maillard-reaction: investigation of the chemical strcuture of melanoidins synthesized from D-xylose/glycine using ^{13}C- and ^{15}N-specifically labeled reactants. *J. Carbohydr. Chem.* **1987**, *6*, 87–104.

(23) Ames, J. M. EU COST action 919: melanoidins in food and health. *Int. Congr. Ser.* **2002**, *1245*, 389−390 (2).

(24) Feather, M. S.; Huang, R.-D. Maillard polymers derived from D-glucose-1 and D-glucose-6-C-14, glycine-1 and glycine-2-C-14, and, C-1-methionine, and methyl-C-14-methionine. *J. Carbohydr. Chem.* **1985**, 4.

(25) Hedges, J. I. The formation and clay mineral reactions of melanoidins. *Geochim. Cosmochim. Acta* **1978**, *42*, 69–76.

(26) Dixon, W. T. NMR spectra in spinning samples. *J. Chem. Phys.* **1982**, *77*, 1800–1809.

(27) Bennett, A. E.; Rienstra, C. M.; Auger, M.; Lakshmi, K. V.; Griffin, R. G. Heteronuclear decoupling in rotating solids. *J. Chem. Phys.* **1995**, *103*, 6951–6958.

(28) Mao, J.-D.; Hu, W.-G.; Schmidt-Rohr, K.; Davies, G.; Ghabbour, E. A.; Xing, B. Quantitative characterization of humic substances by solid-state carbon-13 nuclear magnetic resonance. *Soil Sci. Soc. Am. J.* **2000**, *64*, 873–884.

(29) Liu, S. F.; Mao, J. D.; Schmidt-Rohr, K. A robust technique for two-dimensional separation of undistorted chemical-shift anisotropy powder patters in magic-angle-spinning NMR. *J. Magn. Reson.* **2002**, *155*, 15–28.

(30) Mao, J.-D.; Schmidt-Rohr, K. Methylene spectral editing in solid-state ^{13}C NMR by three-spin coherence selection. *J. Magn. Reson.* **2005**, *176*, 1–6.

(31) Schmidt-Rohr, K.; Spiess, H. W. *Multidimensional Solid-State NMR and Polymers*; Academic Press: San Diego, CA, 1999.

(32) Duncan, T. M. *A Compilation of Chemical Shift Anisotropies*l Farragut: Chicago, IL, 1997.